Myocilin, a Component of a Membrane-Associated Protein Complex Driven by a Homologous Q-SNARE Domain

ARTICLE *in* BIOCHEMISTRY · MARCH 2012

Impact Factor: 3.02 · DOI: 10.1021/bi300073r · Source: PubMed

3 AUTHORS, INCLUDING:

Brian S Mckay
The University of Arizona
35 PUBLICATIONS **839** CITATIONS

SEE PROFILE

Published in final edited form as:
Biochemistry. 2012 May 1; 51(17): 3606–3613. doi:10.1021/bi300073r.

Myocilin, a Component of a Membrane-Associated Protein Complex Driven by a Homologous Q-SNARE Domain

W. Michael Dismuke[1], **Brian S. McKay**[1,2], and **W. Daniel Stamer**[3]

[1]Ophthalmology & Vision Science, University of Arizona, Tucson, AZ

[2]Cell Biology and Anatomy, University of Arizona, Tucson, AZ

[3]Ophthalmology, Duke University, Durham, NC

Abstract

Myocilin is a widely expressed protein with no known function, however, mutations in myocilin appear to manifest uniquely as ocular hypertension and the blinding disease glaucoma. Using the protein homology/analogy recognition engine (PHYRE) we find that the olfactomedin domain of myocilin is similar in sequence motif and structure to a six-bladed, kelch repeat motif based on the known crystal structures of such proteins. Additionally, using sequence analysis we identify a coiled-coil segment of myocilin with homology to human Q-SNARE proteins. Using COS-7 cells expressing full length human myocilin and a version lacking the C-terminal olfactomedin domain, we identified a membrane-associated protein complex containing myocilin by hydrodynamic analysis. The myocilin construct that included the coiled-coil but lacked the olfactomedin domain formed complexes similar to the full-length protein, indicating that the coiled-coil domain of myocilin is sufficient for myocilin to bind to the large detergent resistant complex. In human retina and retinal pigment epithelium, which express myocilin, we detected the protein in a large, SDS-resistant, membrane-associated complex. We characterized the hydrodynamic properties of myocilin in human tissues as either a 15s complex with an M_r=405,000–440,000 yielding a slightly elongated globular shape similar to known SNARE complexes or a dimer of 6.4s and Mr=108,000. By identifying the Q-SNARE homology within the second coil of myocilin and documenting its participation in a SNARE-like complex, we provide evidence of a SNARE domain containing protein associated with a human disease.

Myocilin is a 504 amino acid protein, widely expressed in human and mammalian tissues that differ greatly in function and cell type (1–3), yet the function of myocilin remains unknown. Myocilin is composed of three independent folding domains; an amino terminal helix-turn-helix (hth), a central coiled-coil (CC) and a large hydrophobic carboxy terminal domain with homology to olfactomedin (OLF) (4). Previous studies have demonstrated that myocilin exists as a dimer and by using mutational analysis showed dimerization is mediated through hydrophobic residues within the coiled-coil region (5). Rotary shadowing confirmed dimerization of the coiled-coil region, with a parallel arrangement, suggesting a similar orientation in a myocilin dimer (4).

The three independent folding domains of myocilin contribute to individual trafficking steps as the protein moves from the Golgi apparatus to the plasma membrane. Using protein chimeras containing combinations of the independent folding domains of myocilin fused to GFP the cellular localization was assessed. The hth-CC-GFP chimera, lacking the OLF domain, associated with intracellular vesicles which accumulated at cell boarders, but did

Corresponding Author: W. Daniel Stamer Professor of Ophthalmology Duke University Office: 919-684-3745dan.stamer@duke.edu.

not appear to readily fuse with the plasma membrane. Chimeras of the CC region fused to GFP were targeted to the Golgi apparatus, which became engorged and was lethal to the cells, suggesting inhibition of transport from the Golgi apparatus. Conversely, the hth-GFP chimeras were diffusely distributed in the cytoplasm and excluded from the nucleus. OLF-GFP chimeras were detected in the cytoplasm and nucleus but were also enriched at the plasma membrane (4). In summary, the CC domain appeared to target the constructs to the secretory compartment, and this was lethal in the absence of the hth domain. The OLF domain appeared to have no targeting information, but in its absence, the constructs lead to build up of large vesicles suggesting impaired fusion with the plasma membrane.

Sequence analysis of the myocilin hth or CC domains does not indicate either would have an innate capacity to associate with membranes, yet the hth-CC-GFP chimera as well as the CC-GFP chimera associate with the vesicular compartment. We hypothesize that myocilin associates with cellular membranes via protein-protein interactions mediated through its CC region. Here we characterize membrane associated myocilin from two tissues that express the protein endogenously and COS-7 cells expressing GFP chimeras of myocilin constructs. To do this we use sequence analysis, western blotting and three stringent, complementary biochemical methods; density and velocity gradient sedimentation and size-exclusion chromatography.

Materials and Methods

Membrane preparation

Human donor eyes with no history of ocular disease or surgery were obtained from Banner Sun Health (Sun City, Arizona) within 24–36 hours after death. Briefly, eyes were hemisected and the vitrous was removed. The retina was removed and placed in a hypotonic lysis buffer (5mM N-ethylmaleide, 10mM EDTA, pH 7.4). The RPE cells were then carefully harvested, as described previously(6), by scraping the cells with a scalpel blade and depositing them in hypotonic lysis buffer. Similarly, COS-7 transfected with the N-terminal portion of myocilin (hth-CC) fused to GFP, described previously (4),were harvested in the hypotonic lysis buffer. The tissues or cells were homogenized in a Dounce homogenizer on ice (40 strokes). Nuclei were pelleted at 1,000×g for 1 minute. The resulting supernatant was loaded onto a 1M sucrose cushion and centrifuged at 20,000×g, 4°C for 1 hour using a FA-45-24-11 rotor (Eppendorf, Germany). The supernatant was collected, centrifuged at 25,000×g, 4°C for 10 minutes and the resulting supernatant (soluble fraction) was stored at 4°C. The pelleted membrane fraction was resuspended in hypotonic lysis buffer and pelleted at 25,000×g, 4°C for 10 minutes. The resulting pellet (membrane fraction) was resuspended in 200μL hypotonic lysis buffer and stored at 4°C.

Western blotting and Silver Staining

Polyclonal rabbit anti-myocilin antibodies were produced and previously characterized by our laboratory (7). Proteins were separated on 10% SDS-PAGE gels, transferred electrophoretically to nitrocellulose membranes and blocked in Tris-buffered saline, 0.2% Tween 20 (TBST) with 5% nonfat dry milk. Rabbit anti-myocilin antibodies were added and blots were gently agitated overnight at 4°C. Membranes were washed in TBST, 3 times for 20 minutes, incubated with anti-rabbit horseradish peroxidase-conjugated secondary antibodies (Jackson ImmunoResearch Labortories, Inc. ,West Grove, PA) in TBST for 1 hour and washed with TBST 3 times for 10 minutes. Enhanced chemiluminescence (ECL) (Amersham Biosciences) and X-ray film (Phenix Research Products, Belgium) were used to visualize protein-antibody complexes. For silver staining, protein standards (GE healthcare, Buckinghamshire, UK) were separated by SDS-PAGE and stained using a Bio-Rad silver stain kit per the manufactures instructions.

Gradient sedimentation

SDS was added to membrane and soluble preparations of human RPE and retina to a final concentration of 0.1%. The membrane and soluble preparations were then centrifuged for 1hr @ 25,000×g to remove any insoluble material. The resulting solubilized fractions were layered onto either a linear glycerol gradient (10–40%) or linear sucrose gradient (0.5–2.5M). Linear gradients were produced using the Gradient Master 107ip (BioComp Instruments Inc., Fredericton, Canada) per manufactured directions. Gradients were centrifuged at 100,000×g, 25°C for 2 hours using a TLS-55 rotor (Beckman Coulter, USA). Fractions were collected from the top and analyzed for sucrose or glycerol content by refractometry. SDS-PAGE coupled with Western blotting was used to detect myocilin content in the gradient fractions. All experiments were performed in triplicate for both human retina and RPE samples. Svedberg markers run in a separate gradient were aldolase, conalbumin, ferritin and thyroglobulin proteins from GE Healthcare (Buckinghamshire, UK).

Gel Filtration

SDS solubilized membrane fractions (200μL), described above, were loaded onto a 1 × 50cm gel exclusion column (Bio-Rad Laboratories, Hercules, CA) prepared with a mixed beads resin consisting of sephadex S200 and S400 beads (Amersham Biosciences, Uppsala, Sweden)(1:1) equilibrated with phosphate buffered saline. Fractions were collected and myocilin content was detected by western blot as described above.

Molecular Modeling and Homology Analysis

Protein sequences were obtained from the NCBI protein database. Alignments were generated using CLUSTALW (8). Sequences were input to the protein homology/analogy recognition engine (PHYRE) version 0.2 (http://www.sbg.bio.ic.ac.uk/phyre/).

Results

Molecular modeling of the olfactomedin domain of human myocilin

The crystal structure of myocilin has not been determined. To generate models of myocilin's independent folding domains we used the Phyre algorithm (9). The Phyre algorithm did not find a homology match to the hth region with high confidence. Conversely, the Phyre algorithm returned high homology matches for the OLF domain of human myocilin. The predicted structure is a six-bladed beta-propeller, with similarity to the kelch domain of human kelch-like protein 12 (klhl12)(e value=0.024, 95% estimated precision). Figure 1A shows a model of the human OLF domain threaded over the second to sixth blade of the klhl12 crystal structure. The first blade of the klhl12 propeller has 3 beta sheets consisting of 42 residues where as myocilin has 25 residues predicted to contain 2 beta sheets and therefore the first blade of the myocilin OLF domain could not be threaded over the klhl12 crystal structure and is not shown in the model. To determine whether the predicted six bladed propeller structure is the likely structure of the OLF domain of myocilin, all of the olfactomedin domains from the 12 known human olfactomedin domain containing proteins (not including myocilin) were analyzed using the Phyre algorithm. The algorithm predicted six bladed propeller structures with high estimated precisions (>90%) and low e-values (0.1105±0.0762, mean±SD) for 11 of the olfactomedin domains. The olfactomedin domain of olfactomedin 4 however was predicted to form a 7 bladed beta propeller structure, but with only 70% estimated precision and 1.1 E-value. Alignments of all 13 of these olfactomedin domain containing proteins show several conserved residues as well as a number of highly similar residues, all of which are predicted to be contained with the anti-parallel beta sheets of the individual blades in the model (Figure 1B).

The coiled-coil segment of myocilin has homology to Q-SNAREs

The Phyre algorithm returned results showing the coiled-coil region to have high structural homology to a number of coiled-coil proteins. Our model and previous results (4) suggests that the coiled-coil segment of myocilin contains a flexible region at amino acids 111–117, separating the segment into two interrupted helices. Analysis of the hydrophobicity in the first coil (amino acids 73–110) shows a disordered distribution of hydrophobic residues that do not appear to fit the traditional pattern of the heptad repeats found in other well described Leucine zipper containing proteins. On the contrary, the location of hydrophobic residues within the second coil (amino acids 118–186) form a traditional heptad repeat sequence common among Leucine zipper domains. When the hydrophobic stripe of the second coil was examined more closely, it was found to contain a glutamine (figure 2A.). The positioning of this glutamine within the hydrophobic stripe of a coiled-coil is highly similar to conserved sequences found in proteins that form SNARE complexes (10) (termed Q-SNARES for the glutamine residue)(11).

Membrane fusion is mediated by SNARE proteins (12, 13). The SNARE complexes responsible for driving fusion of membranes consist of parallel, four helix bundles with an interior layer of mostly hydrophobic residues (14). Highly conserved within these hydrophobic layers are hydrophilic glutamine and arginine residues, designated the “0” layer (15). Aligning the second coil of the CC region of human myocilin with other well characterized human Q-SNARE proteins shows that myocilin has homologous residues at the −5, −1, +1, +2 and +7 positions (Figure 2B.). The homology at these positions is of interest as the residues at the −1, +1 and +2 positions are highly conserved across SNARE motifs and are thought to be of critical importance in shielding the salt bridge formed between the three glutamines and single arginine residue at the 0 layer from the aqueous environment (11). Interestingly, at positions −4, −2, +4, +6 and +8, myocilin contains acidic residues not seen in other characterized human Q-SNARE proteins. If these residues within the second coil of myocilin are of any functional importance, they should be well conserved across mammalian species. Figure 2C shows that indeed, residues important for SNARE complex formation, including these potentially critical residues are well conserved across human, mouse, rat, dog, bovine and pig.

Myocilin exists in two cellular pools by hydrodynamic analysis

The hydrodynamic properties of membrane-associated myocilin were examined in membrane fractions from COS-7 cells expressing full-length myocilin fused to GFP, which were described previously. First, soluble and membrane samples were prepared and solubilized in 0.1% SDS. Resistance to the dissociating effects of ionic detergents, like SDS, is a feature of coiled-coil mediated protein-protein interaction, such as those seen in SNARE complexes (16). The samples were then separated on linear (10–40%) glycerol gradients. Fractions were collected, separated by SDS-PAGE and myocilin was identified by western blot. Membrane-associated, myocilin-GFP chimeras separated into two pools, fractions #1–5 and 14 (Figure 3A). We attempted to establish an S value for the myocilin-GFP construct but due to the inability of the construct to separate through the initial length of the gradient we were unable to. Next, to determine whether the coiled-coil region of myocilin is sufficient to target myocilin to the large membrane associated protein complex, we expressed the hth-CC-GFP protein chimera, which lacks the C-terminal OLF domain, in COS-7 cells. This hth-CC-GFP chimera was previously shown to localize to the membrane fraction (4). Membrane fractions from these cells were prepared and separated over linear (10–40%) glycerol gradients. Figure 3B shows that like the myocilin-GFP construct, the hth-CC-GFP chimera sediments into two pools at 6.2S and 16.3S. Finally, to verify that myocilin constructs detected in higher number fractions were in solution and not an insoluble precipitate, we reduced the centrifugation time by 30 minutes which shifted the

high velocity pool from fraction #14 to fraction #10 (Figure 3C) while retaining the same relationship to the control proteins.

To determine whether endogenous myocilin from human tissue exists in a large, membrane associated protein complex, the hydrodynamic properties of the protein were examined in soluble and membrane fractions from both human retinas and RPE, two tissues known to express the protein. Retinas and RPE were separately dissected from human donor eyes. Soluble and membrane samples of the individual tissues were prepared, solubilized in 0.1% SDS and separated on linear sucrose gradients. In soluble preparations, myocilin separated into lower density fractions exclusively while in membrane preparations myocilin separated into both low density fractions and a high density fraction (fraction #14) (Figure 4A). To determine the sedimentation values for these two pools of myocilin, retina and RPE membrane and soluble preparations were separated in linear glycerol gradients. Myocilin from both retina and RPE membrane preparations (Figure 4B & C) sedimented at 6.4 S and 15 S, likely representing the dimer and large complex, respectively, whereas myocilin from RPE and retina soluble fractions separated at 6.4 S exclusively (not shown). Next we determined the size of the membrane-associated myocilin complex in retina membrane samples by gel exclusion chromatography. Fractions were collected, separated by SDS-PAGE and analyzed by western blot. Figure 5 shows myocilin separating at a peak M_r=405,000–440,000. The myocilin detected at M_r=108,000 likely represents the dimer since monomeric myocilin has a calculated mass of 55–57kDa and myocilin is known to form dimers.

Sedimentation values and size exclusion data allow for a calculation of the shape of both the putative myocilin dimer and myocilin containing complex. The putative myocilin dimer is globular with a S_{max}/S=1.28. The myocilin containing protein complex has a slightly different shape that is roughly globular to slightly elongated with a calculated S_{max}/S ranging from 1.32 to 1.39. This elongated shape has been noted in other detergent resistant proteins complexes mediated by SNARE interactions (Table 1).

Discussion

Here we provide evidence that endogenous myocilin is a component of a large membrane associate complex in two human tissues. Using the computer modeling and sequence analysis we predict the olfactomedin domain of myocilin to have a β-propeller structure and show that a region of the coiled-coil segment has Q-SNARE homology. Our hydrodynamic analysis detected both a putative myocilin dimer and a large complex in the presence of 0.1% SDS. The sedimentation value and M_r for the complex(s) were 15S and 405,000–440,000 yielding a S_{max}/S from 1.32 to 1.39 indicative of an elongated, globular shape, consistant with known SNARE complexes. Hydrodynamic analysis of a protein chimera containing the N-terminal, Q-SNARE-like portion of myocilin confirmed results obtained with endogenous human myocilin; sedimentation in a large SDS-resistant protein complex.

In our analysis of the OLF domain of myocilin using the Phyre algorithm, we observed a number of similar structural predictions for the OLF domain; multi-bladed β-propellers. Our model for the OLF domain in myocilin is based on the highest probability structural match, a six-bladed β-propeller kelch repeat domain. This predicted model is consistent with previous experimental data on the olfactomedin domain showing it to be globular and composed primarily of β-sheets based on CD spectroscopy (17, 18). Additionally, we used the Phyre algorithm to predict to the folding of the olfactomedin domains of the other human proteins that contain this domain. Of the 13 known human proteins with identified olfactomedin domains, all except olfactomedin 4 were predicted to fold into 6 bladed beta propellers with high estimated precision.

The consistent predictions of a beta-propeller structure for the olfactomedin domain, including the OLF in myocilin, are notable as another glaucoma-associated protein, WDR-36, is predicted to contain two beta-propellers. A recent study of the WDR-36 protein demonstrated an interaction between it and the GPCR, thromboxane A2 beta-isoform (19). Since our previous work found the OLF domain of human myocilin alone, enriched at cell borders and kelch repeat motifs like the one found in myocilin, have been shown to bind to GPCRs (20) it is possible that the OLF domain of myocilin ties the protein to a ligand mediated signaling event. Future studies will test this hypothesis.

The majority of glaucoma related mutations in myocilin occur in the OLF domain and since the crystal structure of myocilin has not been determined, our predicted kelch repeat structure will serve as a valuable tool to analyze of the impact of these mutations on folding and biochemical properties. For example, the myocilin OLF mutation that showed the greatest impact on melting temperature in Burns, JN *et al*, 2010 (21), K423E, we predict to be in linking region between blades 4 and 5 and on the exterior portion of the domain where the substitution of a larger basic residue for a smaller acidic one may alter stability. The D380A mutation, which had the least impact on melting temperature, we predict to be in the middle of a beta strand in the 4th blade of the model, flanked by two hydrophobic residues (I379 and L381) and adjacent to two other hydrophobic residues (V328 and V329) where a substitution to a hydrophobic residue may have a negligible impact on stability. These are just a few examples demonstrating the value our model has in the analysis of protein folding and stability resulting from amino acid substitutions in the OLF domain.

Our data suggests that myocilin is a member of a large, membrane-associated protein complex with binding between myocilin and the other members of the complex mediated by coiled-coil interactions. The formation of this protein complex with myocilin constructs lacking the OLF domain as well as complex stability, unheated in 0.1% SDS demonstrates that this myocilin protein-protein interaction involves the coiled-coil containing N-terminal portion of the protein but not the C-terminal OLF domain. Our previous work using rotary shadowing illustrates that the CC domain of myocilin is composed of two helices separated by a short flexible linker (4). While the first coil has a number of hydrophobic residues, they do not resemble a leucine zipper motif, as does the second coil. The leucine zipper motif of the second coil alone should be capable of forming multi-coiled structures, but our analysis of this region revealed a number of notable features which are reminiscent of the well characterized SNARE proteins. These features include an alpha helix that is the proper length (approximately 68 residues), characteristic hydrophilic glutamine residue imbedded within the hydrophobic stripe to form a salt bridge and the highly conserved hydrophobic residues at the −1, +1 and +2 positions (10). The presence of these characteristic features in myocilin supports the idea of Q-SNARE homology within the CC region.

The myocilin-containing protein complex(s) has a number of properties found in other protein complexes where a SNARE core mediates oligimerization. First, the myocilin containing protein complex remains intact in the presence of 0.1% SDS. Resistance to the dissociating effects of ionic detergents is a key feature found in protein complexes formed by coiled-coil associations such as in SNARE complexes (16). Second, our hydrodynamic analysis of the complex revealed a size and importantly, a shape similar to other known SNARE complexes. The first SNARE complex described was the membrane-associated, detergent-extracted “20s fusion particle” (22). The fusion particle was eventually shown to contain the SNARE proteins SNAP-25, syntaxin and synaptobrevin-2 (23). The 20s, 700kDa complex has a similar, oblong shape to the myocilin containing complex we have identified (S_{max}/S = 1.42 versus 1.32 to 1.39, respectively) (Table 1).

Another feature myocilin seems to share with other SNARE proteins is an amino terminal regulatory domain. Our previous work demonstrated the subcellular localization of various GFP fusion proteins made from combinations of the three independent folding domains of myocilin (4). There we showed the coiled-coil region of myocilin localized to the Golgi apparatus which is consistent with our findings here of endogenous myocilin associating with membranes. In those studies the coiled-coil construct proved to be lethal, probably due to a blockage of vesicle formation from the Golgi apparatus. When the amino-terminal hth region was included with the CC region, the hth-CC chimera associated with numerous vesicles that accumulated at the plasma membrane. These results suggest that the hth region facilitates proper budding of myocilin-associated vesicles from the Golgi apparatus. Notably, several SNARE proteins have been shown to have amino-terminal regulatory domains thought to facilitate proper SNARE complex formation including the Habc domain of Vtilb and all syntaxins (24–27), the PX domain of Vam7P(28) and the longin domain of Sec22b (29), Ykt6(30) and VAMP7(31). Future studies will have to determine whether the hth region of myocilin performs a similar role.

Our findings suggest that myocilin associates with cellular membranes via a coiled-coil mediated protein-protein interaction. Myocilin's coiled-coil region has homology to known Q-SNAREs and the membrane associated protein complex containing myocilin has hydrodynamic properties similar to known SNARE complexes. Further, our data suggest functions for the two other domains in a regulated secretory process, the N-terminal HTH domain may be a regulatory domain necessary for vesicle formation and the olfactomedin domain with its kelch-like properties may interact with GPCR's at the plasma membrane. With this in mind, our findings suggest that a dysfunction in vesicle trafficking or homeostasis is at the root of primary open angle glaucoma. Myocilin is expressed in numerous tissues of the body (32) yet the only observed phenotype associated with myocilin mutations is ocular hypertension and primary open-angle glaucoma. The next step toward understanding both the role myocilin plays in cellular physiology and how mutations in myocilin manifest as POAG, is to identify the other components of the myocilin associate SNARE-like complex illustrated in this study. By identifying these unknown components and examining their properties we will be closer to understanding processes critical for proper regulation of intraocular pressure at an intracellular level.

Acknowledgments

The authors thank the members of the International Lions Club for all of their help transporting donor tissue and for their kind donations to the Ophthalmology Department.

Supported: unrestricted grant from Research to Prevent Blindness, NEI grant EY012797 and the Interdisciplinary Training in Cardiovascular Research grant HL07249.

Abbreviations

Hth	helix turn helix
CC	coiled-coil
OLF	olfactomedin
GFP	green fluorescent protein
RPE	retinal pigment epithelium
SNARE	Soluble NSF attachment protein receptor
GPCR	G-protein coupled receptor

POAG primary open angle glaucoma

References

(1). Fingert JH, Ying L, Swiderski RE, Nystuen AM, Arbour NC, Alward WL, Sheffield VC, Stone EM. Characterization and comparison of the human and mouse GLC1A glaucoma genes. Genome Res. 1998; 8:377–384. [PubMed: 9548973]

(2). Ortego J, Escribano J, Coca-Prados M. Cloning and characterization of subtracted cDNAs from a human ciliary body library encoding TIGR, a protein involved in juvenile open angle glaucoma with homology to myosin and olfactomedin. FEBS letters. 1997; 413:349–353. [PubMed: 9280311]

(3). Nguyen TD, Chen P, Huang WD, Chen H, Johnson D, Polansky JR. Gene structure and properties of TIGR, an olfactomedin-related glycoprotein cloned from glucocorticoid-induced trabecular meshwork cells. The Journal of biological chemistry. 1998; 273:6341–6350. [PubMed: 9497363]

(4). Stamer WD, Perkumas KM, Hoffman EA, Roberts BC, Epstein DL, McKay BS. Coiled-coil targeting of myocilin to intracellular membranes. Experimental eye research. 2006; 83:1386–1395. [PubMed: 16973161]

(5). Fautsch MP, Johnson DH. Characterization of myocilin-myocilin interactions. Investigative ophthalmology & visual science. 2001; 42:2324–2331. [PubMed: 11527946]

(6). Burke JM, McKay BS, Jaffe GJ. Retinal pigment epithelial cells of the posterior pole have fewer Na/K adenosine triphosphatase pumps than peripheral cells. Invest Ophthalmol Vis Sci. 1991; 32:2042–2046. [PubMed: 1647375]

(7). Stamer WD, Roberts BC, Howell DN, Epstein DL. Isolation, culture, and characterization of endothelial cells from Schlemm's canal. Investigative ophthalmology & visual science. 1998; 39:1804–1812. [PubMed: 9727403]

(8). Chenna R, Sugawara H, Koike T, Lopez R, Gibson TJ, Higgins DG, Thompson JD. Multiple sequence alignment with the Clustal series of programs. Nucleic acids research. 2003; 31:3497–3500. [PubMed: 12824352]

(9). Kelley LA, Sternberg MJ. Protein structure prediction on the Web: a case study using the Phyre server. Nature protocols. 2009; 4:363–371.

(10). Weimbs T, Low SH, Chapin SJ, Mostov KE, Bucher P, Hofmann K. A conserved domain is present in different families of vesicular fusion proteins: a new superfamily. Proceedings of the National Academy of Sciences of the United States of America. 1997; 94:3046–3051. [PubMed: 9096343]

(11). Fasshauer D, Sutton RB, Brunger AT, Jahn R. Conserved structural features of the synaptic fusion complex: SNARE proteins reclassified as Q- and R-SNAREs. Proceedings of the National Academy of Sciences of the United States of America. 1998; 95:15781–15786. [PubMed: 9861047]

(12). Sollner T, Bennett MK, Whiteheart SW, Scheller RH, Rothman JE. A protein assembly-disassembly pathway in vitro that may correspond to sequential steps of synaptic vesicle docking, activation, and fusion. Cell. 1993; 75:409–418. [PubMed: 8221884]

(13). Weber T, Zemelman BV, McNew JA, Westermann B, Gmachl M, Parlati F, Sollner TH, Rothman JE. SNAREpins: minimal machinery for membrane fusion. Cell. 1998; 92:759–772. [PubMed: 9529252]

(14). Antonin W, Fasshauer D, Becker S, Jahn R, Schneider TR. Crystal structure of the endosomal SNARE complex reveals common structural principles of all SNAREs. Nature structural biology. 2002; 9:107–111.

(15). Sutton RB, Fasshauer D, Jahn R, Brunger AT. Crystal structure of a SNARE complex involved in synaptic exocytosis at 2.4 A resolution. Nature. 1998; 395:347–353. [PubMed: 9759724]

(16). Hayashi T, McMahon H, Yamasaki S, Binz T, Hata Y, Sudhof TC, Niemann H. Synaptic vesicle membrane fusion complex: action of clostridial neurotoxins on assembly. The EMBO journal. 1994; 13:5051–5061. [PubMed: 7957071]

(17). Orwig SD, Lieberman RL. Biophysical characterization of the olfactomedin domain of myocilin, an extracellular matrix protein implicated in inherited forms of glaucoma. PloS one. 2011; 6:e16347. [PubMed: 21283635]

(18). Nagy I, Trexler M, Patthy L. Expression and characterization of the olfactomedin domain of human myocilin. Biochemical and biophysical research communications. 2003; 302:554–561. [PubMed: 12615070]

(19). Cartier A, Parent A, Labrecque P, Laroche G, Parent JL. WDR36 acts as a scaffold protein tethering a G-protein-coupled receptor, Galphaq and phospholipase Cbeta in a signalling complex. J Cell Sci. 124:3292–3304. [PubMed: 21940795]

(20). Rondou P, Haegeman G, Vanhoenacker P, Van Craenenbroeck K. BTB Protein KLHL12 targets the dopamine D4 receptor for ubiquitination by a Cul3-based E3 ligase. The Journal of biological chemistry. 2008; 283:11083–11096. [PubMed: 18303015]

(21). Burns JN, Orwig SD, Harris JL, Watkins JD, Vollrath D, Lieberman RL. Rescue of glaucoma-causing mutant myocilin thermal stability by chemical chaperones. ACS chemical biology. 2010; 5:477–487. [PubMed: 20334347]

(22). Wilson DW, Whiteheart SW, Wiedmann M, Brunner M, Rothman JE. A multisubunit particle implicated in membrane fusion. The Journal of cell biology. 1992; 117:531–538. [PubMed: 1315316]

(23). Sollner T, Whiteheart SW, Brunner M, Erdjument-Bromage H, Geromanos S, Tempst P, Rothman JE. SNAP receptors implicated in vesicle targeting and fusion. Nature. 1993; 362:318–324. [PubMed: 8455717]

(24). Antonin W, Dulubova I, Arac D, Pabst S, Plitzner J, Rizo J, Jahn R. The N-terminal domains of syntaxin 7 and vti1b form three-helix bundles that differ in their ability to regulate SNARE complex assembly. The Journal of biological chemistry. 2002; 277:36449–36456. [PubMed: 12114520]

(25). Fernandez I, Ubach J, Dulubova I, Zhang X, Sudhof TC, Rizo J. Three-dimensional structure of an evolutionarily conserved N-terminal domain of syntaxin 1A. Cell. 1998; 94:841–849. [PubMed: 9753330]

(26). Munson M, Chen X, Cocina AE, Schultz SM, Hughson FM. Interactions within the yeast t-SNARE Sso1p that control SNARE complex assembly. Nature structural biology. 2000; 7:894–902.

(27). Dulubova I, Yamaguchi T, Wang Y, Sudhof TC, Rizo J. Vam3p structure reveals conserved and divergent properties of syntaxins. Nature structural biology. 2001; 8:258–264.

(28). Cheever ML, Sato TK, de Beer T, Kutateladze TG, Emr SD, Overduin M. Phox domain interaction with PtdIns(3)P targets the Vam7 t-SNARE to vacuole membranes. Nature cell biology. 2001; 3:613–618.

(29). Gonzalez LC Jr. Weis WI, Scheller RH. A novel snare N-terminal domain revealed by the crystal structure of Sec22b. The Journal of biological chemistry. 2001; 276:24203–24211. [PubMed: 11309394]

(30). Tochio H, Tsui MM, Banfield DK, Zhang M. An autoinhibitory mechanism for nonsyntaxin SNARE proteins revealed by the structure of Ykt6p. Science. 2001; 293:698–702. [PubMed: 11474112]

(31). Rossi V, Banfield DK, Vacca M, Dietrich LE, Ungermann C, D'Esposito M, Galli T, Filippini F. Longins and their longin domains: regulated SNAREs and multifunctional SNARE regulators. Trends in biochemical sciences. 2004; 29:682–688. [PubMed: 15544955]

(32). Tamm ER. Myocilin and glaucoma: facts and ideas. Progress in retinal and eye research. 2002; 21:395–428. [PubMed: 12150989]

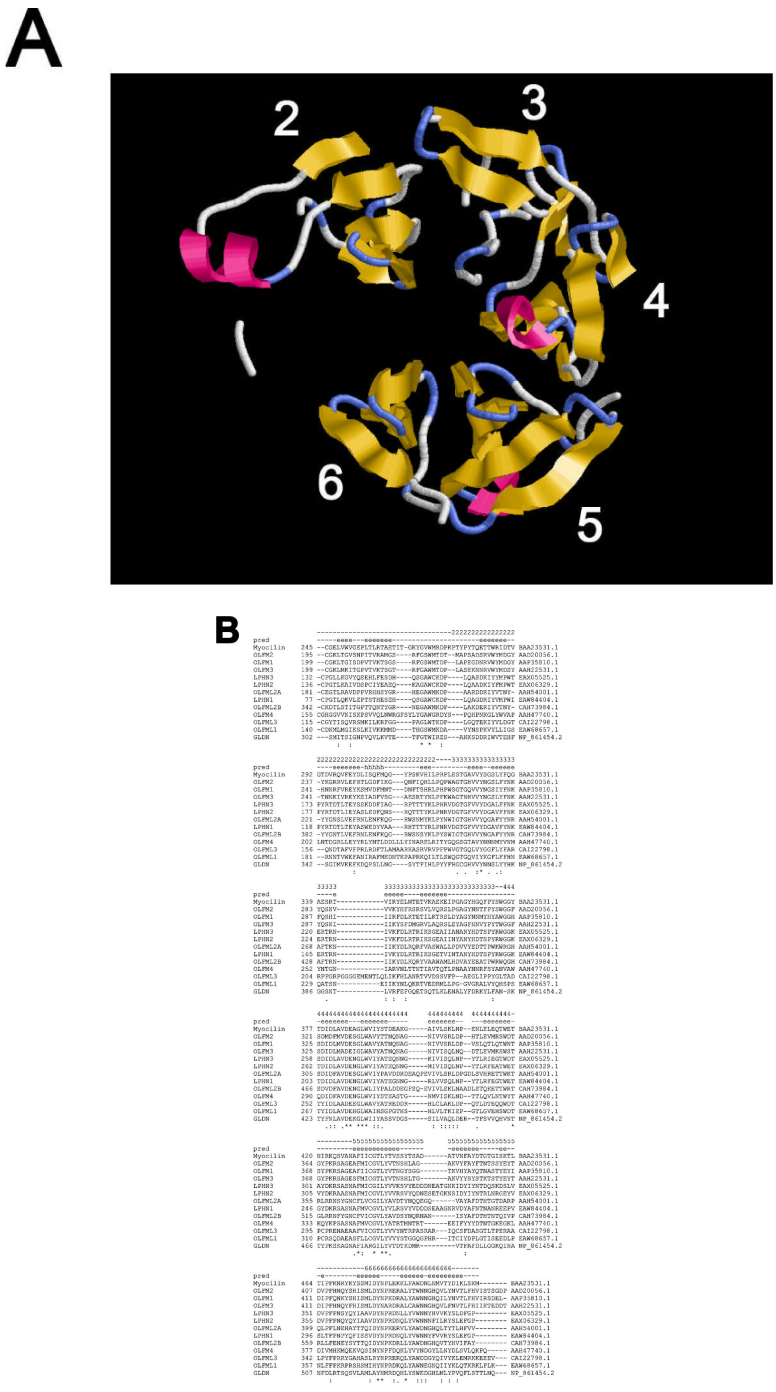

Figure 1.

The three-dimensional structure of the olfactomedin domain of myocilin by homology modeling. The Phyre algorithm predicted with high precision a six-bladed, beta propeller folding, most similar to a kelch motif, for the OLF domain of myocilin. Ribbon model of proposed structure of myocilin OLF domain with individual blades numbered (A). The model is colored based on structure. Yellow=beta sheets, magenta=helix, blue=beta turns. Alignment of known olfactomedin domains from human olfactomedin domain containing proteins using ClustalW (B). Numbers listed above the alignment represent location of those residues within the proposed model. “Pred” indicates secondary structure consensus as

calculated by Phyre for the myocilin OLF domain. The olfactomedin domains from the known olfactomedin domain containing human proteins were analyzed using the Phyre algorithm and all but one, the olfactomedin domain form olfactomedin 4 (AAH47740.1), returned high precision matches to six-bladed, beta propeller folds.

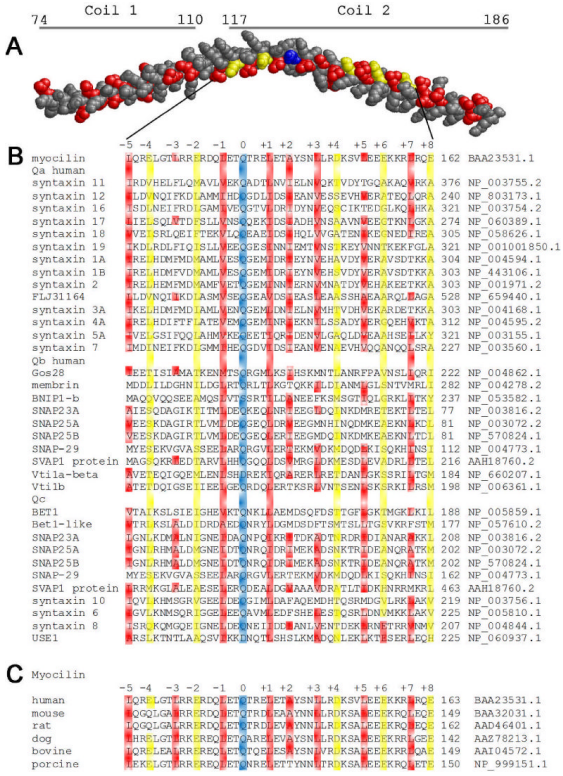

Figure 2.

Analysis of the coiled-coil region of human myocilin. The Phyre algorithm generated a model of the CC region of myocilin (aa 73–186)(A). Hydrophobic residues are colored in red. The glutamine residue in the central “0” layer of the second coil is colored blue while the acidic residues at the −4, −2, +4, +6 and +8 positions are colored yellow. Clearly visible in the second coil (aa 118–186) is a hydrophobic stripe. The amino acid sequence contained within the second coil is compared to all known human Q-SNARE motifs (B). The hydrophobic residues at the −1, +1 and +2 position are well conserved between human myocilin and known Q-SNAREs. The Q-SNARE motif is also well conserved across the known mammalian myocilin sequences (C).

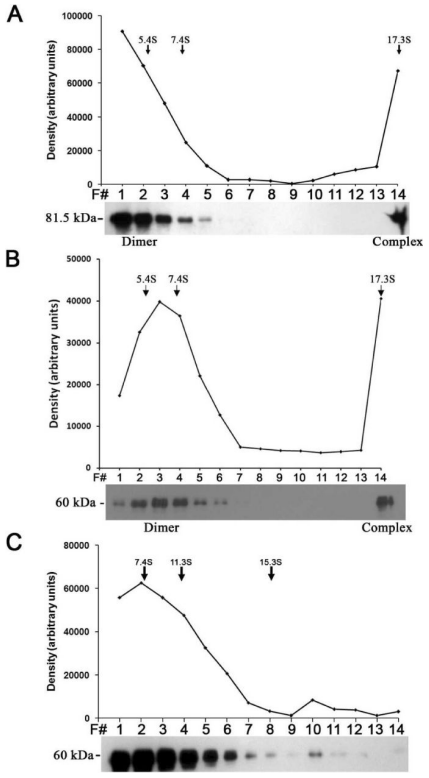

Figure 3.

Identification of a large, membrane-associated protein complex containing myocilin by velocity gradient sedimentation. COS-7 cells expressing GFP fused to full length myocilin or myocilin lacking the OLF domain were homogenized and fractionated into soluble and membrane portions. SDS was added to samples to a final concentration of 0.1% prior to centrifugation on linear (10–40%) glycerol gradients. Fractions were collected, separated by SDS-PAGE and analyzed by western blot for myocilin using anti-myocilin IgGs. Western blots show full-length myocilin (A) and the N-terminal portion of myocilin lacking the OLF domain (B) separate into two distinct pools, representing a dimer and a large protein complex containing myocilin. Reducing the centrifugation times by 30 minutes demonstrates that the myocilin containing complex is in solution and not a pelleted precipitate (hth-CC-GFP chimera shown) (C).

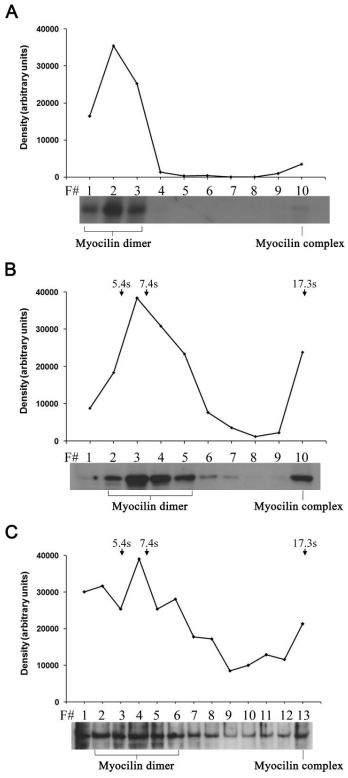

Figure 4.

Analysis of the membrane-associated myocilin complex by velocity gradient sedimentation. Fresh human retinas and RPE were fractionated into soluble and membrane portions. SDS was added to membrane (shown here) and soluble preparations (0.1% final concentration), which were separated on linear sucrose (A) and glycerol (B & C) gradients. Fractions were collected and separated by SDS-PAGE. Western blots (A) show myocilin from human retina membrane preparations separated in a small and large complex on linear sucrose gradients. Similarly, human retina (B) and RPE (C) membrane preparations separated on linear glycerol gradients as both a 6.4s dimer and a larger 15s complex (values are results obtained in three separate experiments for each tissue).

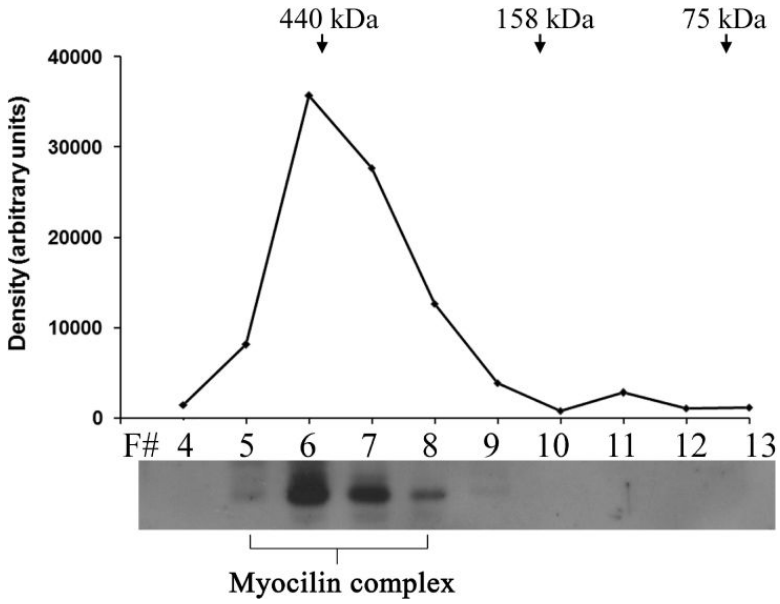

Figure 5.

Analysis of the membrane-associated myocilin complex by gel exclusion chromatography. Fresh human retinas were fractionated into soluble and membrane portions. SDS was added to membrane and soluble preparations (0.1% final concentration). Retina membrane (shown here) and soluble preparations were then separated on a gel exclusion column and myocilin from collected fractions was detected by western blot. Myocilin was detected in a large (M_r=405,000–440,000) complex as well as a smaller (M_r=108,000) dimer. M_r values were calculated from experiments performed in triplicate.

Table 1

Summary of hydrodynamic data obtained by analysis of human myocilin from retina and RPE compared to a known SNARE complex. Sedimentation value and M_r for SNARE complex were obtained from (22).

	S value	M_r	S_{max}/S	Shape
Myocilin dimer	6.4	108,000	1.28	globular
Myocilin complex	15	405,000–440,000	1.32–1.39	globular, slightly elongated
SNARE complex	20	700,000	1.42	globular, slightly elongated